Synergistic NaOH–Ultrasonic Activation of Palm Shell–Derived Carbon for Enhanced Adsorption of Naphthol Yellow Dye

Intan Lestari[1], Sultan Leofayuda[2], Diah Riski Gusti[3], Damris Muhammad[4]

{ilestari_15@unja.ac.id[1], sultanleofayuda@gmail.com[2], diahgusti@unja.ac.id[3], damris@unja.ac.id[4]}

Program Studi of Chemistry, Faculty Science and Technology, Universitas Jambi[1,2,3,4]

Corresponding author: ilestari_15@unja.ac.id

Abstract. Liquid waste of synthetic dyes from textile and batik industries contains dyes such as naphthol which are difficult to degrade naturally, are toxic and have the potential to cause negative impacts on aquatic ecosystems. The manufacture of activated palm shell carbon using NaOH and ultrasonication has been carried out for the absorption of naphthol dyes. The study was conducted by activating carbon with 2M NaOH and physical activation through ultrasonication at a frequency of 40 kHz for 30 minutes. Characterization of activated carbon was carried out through proximate analysis to determine the content of water, ash, volatile, and fixed carbon. Analysis with a Fourier Transform Infrared (FTIR) instrument to identify the functional groups of activated carbon, Scanning Electron Microscopy (SEM) to see the surface morphology and ImageJ software analysis to see the average pore size distribution. FTIR analysis confirmed the presence of functional groups –OH, C-O, and aromatic C=C which play a role in the adsorption process, while SEM results showed a carbon surface with more open pores and increased after activation. The adsorption test of naphthol dye solution showed optimum capacity at pH 4 condition with adsorption capacity of 1.957 mg/g, contact time of 30 minutes with Q = 1.990 and naphthol absorption concentration increased to 300 mg/L with Q = 20.590 mg/g.

Keywords: Activated carbon, palm kernel shell, ultrasonication, adsorption, naphtol.

1 Introduction

Activated carbon (AC) is a highly porous carbonaceous material produced by sequential dehydration, carbonization, and activation steps; these treatments generate materials with very large specific surface areas and extensive pore networks, making AC widely applied as an efficient adsorbent for organic pollutants in water treatment. Activated carbon (AC) derived from biomass has gained increasing attention due to its sustainability, abundance, and cost-effectiveness as an alternative adsorbent for environmental remediation and industrial

SICBAS 2025, November 06, Palembang, Indonesia

DOI 10.4108/eai.6-11-2025.2364451

applications. Biomass precursors—such as agricultural residues and lignocellulosic waste—contain high carbon content and are suitable for conversion into activated carbon, contributing to circular economy practices and waste-to-resource utilization [1]. Enhancing the adsorption capability of activated carbon requires precise control of the surface chemistry and pore structure through the activation method applied.

Palm kernel shell (PKS) has been identified as a promising lignocellulosic precursor for high-performance activated carbon because torrefaction/pyrolysis and subsequent activation of PKS produce materials with large surface area, well-developed micropore–mesopore structures, and useful surface functional groups suitable for adsorption applications [2].

Chemical activation is widely recognized as an efficient route for developing microporous structures and generating a high specific surface area. Activating agents such as KOH, NaOH, H_2SO_4, and $ZnCl_2$ induce carbon matrix cleavage and promote the development of well-distributed pores throughout the carbon surface [1]. The structure can be further optimized using physical activation, typically performed by high-temperature treatment with oxidizing gases or steam. This step stabilizes the carbon structure and expands pore networks, resulting in enhanced adsorption properties [2].

Recent advancements have introduced ultrasonication as a complementary pretreatment or post-treatment step in activated carbon synthesis. Ultrasonic irradiation generates acoustic cavitation, which increases mass transfer, promotes homogeneous diffusion of chemical activating agents, and enhances pore accessibility within the carbon matrix [3][4]. Studies have demonstrated that ultrasound-assisted activation improves pore uniformity, increases surface functionality, and produces activated carbon with superior adsorption capacity [4][5]. Therefore, combining chemical activation, steam-based physical activation, and ultrasonication provides a promising pathway to produce biomass-derived activated carbon with hierarchical porosity and improved performance. Ultrasonic-assisted processing employed either as a pretreatment during chemical impregnation or during adsorption experiments enhances mass transfer through acoustic cavitation, improves dispersion and penetration of activating solutions into the biomass matrix, and can increase pore accessibility and surface cleanliness, leading to improved textural and adsorption properties [5][6].

Synthetic azo dyes (e.g., Naphthol Yellow and other azo class dyes) are widely used in the textile industry for their bright colors and processability; however, their azo chromophores and substituent groups confer high chemical stability and resistance to biodegradation, and many azo dyes and their metabolites pose toxic, mutagenic, or carcinogenic risks to aquatic ecosystems and human health [7].

2 Materials and methods

2.1 Activation of activated carbon

Palm kernel shell (PKS) was used as the carbon precursor. Chemical activation was carried out by impregnating the precursor with 2 M NaOH at a mass ratio of 1:3 (precursor:NaOH). The mixture was stirred and soaked for 24 h to ensure uniform diffusion of the activating agent. NaOH activation enhances pore formation through the cleavage of carbon–oxygen bonds and removal of volatile matter, which increases pore accessibility.

Following impregnation, the sample underwent ultrasonication at 35 W and 40 kHz for 4 h. Ultrasonic cavitation improves the penetration of the activating agent into internal pore structures and accelerates surface cleaning by removing impurities trapped inside the pores [8]. After treatment, the sample was washed with HCl solution followed by distilled water until reaching neutral pH, dried at 110 °C for 60 min, and finally activated in a furnace at 750 °C for 1 h under limited oxygen flow [1].

2.2 Proximate analysis

Proximate analysis of moisture, ash, volatile matter, and fixed carbon was performed following the ASTM D2866-70 standard method. The analysis reflects the purity and adsorptive quality of activated carbon, especially fixed carbon and ash content, which influence adsorption capacity [9].

2.3 Characterization of activated carbon

The activated carbon was characterized using: FTIR: to identify surface functional groups related to adsorption behavior, SEM: to observe pore morphology and surface texture and UV–Vis spectrophotometry: to quantify dye removal efficiency under different operating parameters. FTIR and SEM are widely used to confirm pore development and functional group modifications during activation [10].

2.4 Adsorption experiment

Adsorption studies were performed to investigate the effects of solution pH, contact time, initial dye concentration, and adsorbent dosage on removal efficiency. Effect of pH adsorption: 10 mL Naphthol Yellow solution (25 ppm) was mixed with 0.1 g of activated carbon. The pH was adjusted to pH 4, 5, 6, 7, and 8. Each sample was shaken at 100 rpm for 60 min and filtered, and the residual dye concentration was measured using UV–Vis spectrophotometry. The effects of contact time (30–90 min) and initial dye concentration (50–300 ppm) were also evaluated to determine adsorption behavior.

3 Result and discussion

3.1 Proximate analysis

The proximate analysis of palm shell–based activated carbon under various activation treatments is summarized in **Table 1**. The moisture content decreased sharply from 6.38% in the raw carbon to 0.003% in the NaOH–ultrasonicated sample (C-NaOH-U). This significant reduction indicates that NaOH activation combined with ultrasonication effectively removes physically adsorbed water and volatile compounds, producing a more stable and less hygroscopic carbon structure [11].

The ash content increased from 2.83% in the untreated carbon to 7.56% in the C-NaOH-U sample. Despite the increase, the ash content remained below the maximum allowable limit (<10%) for activated carbon quality based on the SII No. 0258-79 standard, confirming that the material still meets commercial-grade requirements.

Volatile matter exhibited a slight increase after activation. In contrast, the fixed carbon content significantly improved, reaching 99.95% for NaOH-activated carbon and 99.22% for the NaOH–ultrasonicated sample. These values far exceed the minimum quality requirement (>65%), demonstrating highly efficient carbonization and excellent carbon purity, which are desirable for adsorption applications [6].

3.2 Characteristics of activated carbon

3.2.1 Fourier transform infrared (FTIR) analysis

The FTIR spectra of palm shell–based activated carbon obtained under three different activation conditions—untreated carbon (Carbon), NaOH-activated carbon (AC-NaOH), and NaOH–ultrasonicated activated carbon (AC-NaOH-U)—are shown in **Figure 1**. The spectra reveal notable changes in both the intensity and distribution of absorption bands, reflecting the modification of surface functional groups induced by chemical activation and ultrasonication.

A broad absorption band centered at approximately 3343.17 cm^{-1}, corresponding to O–H stretching vibrations of hydroxyl groups and adsorbed moisture, was clearly observed in the untreated carbon. The intensity of this band significantly decreased after NaOH activation and further diminished in the AC-NaOH-U sample, indicating the progressive removal of oxygen-containing polar functional groups during activation. This reduction suggests enhanced dehydration and dehydroxylation reactions, leading to a more hydrophobic carbon surface.

The absorption band at 2918.18 cm^{-1}, assigned to aliphatic C–H stretching vibrations, also showed a marked decrease in intensity after activation. This change implies the decomposition of aliphatic structures and volatile organic components, which is commonly associated with the advancement of the carbonization process. In the region of 1510.11–1593.37 cm^{-1}, corresponding to aromatic C=C stretching vibrations, an increase in band intensity was observed after both NaOH activation and NaOH–ultrasonication. The enhancement of these aromatic signals indicates the development of more condensed aromatic structures and a higher degree of graphitization. This structural evolution is particularly pronounced in the AC-NaOH-U sample, suggesting that ultrasonication facilitates further rearrangement of the carbon framework through cavitation-induced microstructural disruption. Additionally, the bands located in the range of 1036.39–1232.27 cm^{-1}, attributed to C–O stretching vibrations of alcohol, ether, or phenolic groups, exhibited a noticeable reduction in intensity after activation. The decline of these oxygen-containing functional groups further confirms the effective chemical modification of the carbon surface, resulting in increased aromaticity and structural stability [12].

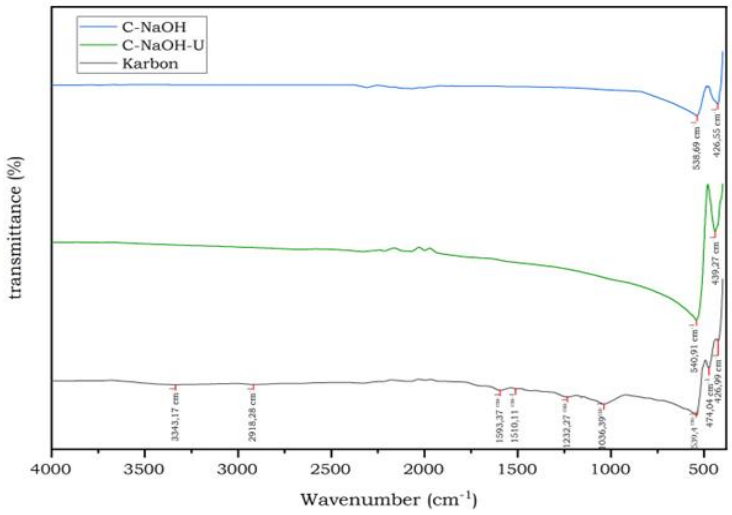

Fig. 1. Spectra FTIR Carbon, AC-NaOH and AC-NaOH-Ultrasonication.

3.2.2 Scanning electron microscopy analysis

The surface morphology of palm shell–based activated carbon under different activation conditions was examined by scanning electron microscopy (SEM), as shown in **Figure 2**. The untreated carbon (**Figure 2a-c**) exhibits a relatively smooth and compact surface with limited visible porosity, indicating incomplete pore development prior to activation.

After NaOH activation (**Figure 2d-f**), the carbon surface becomes noticeably more porous, with the formation of micro-sized pores resulting from alkaline etching and the removal of volatile components. This morphological change confirms the role of NaOH in opening blocked pores and creating new pore structures.

In contrast, the AC-NaOH-U sample (**Figure 2g-i**) displays a rough and heterogeneous surface with well-developed and interconnected pore networks. The enhanced porosity is attributed to the cavitation effect generated during ultrasonication, which intensifies the penetration of the activating agent and promotes more uniform pore formation. These structural transformations indicate a significant increase in surface roughness and accessible pore volume, which are essential factors contributing to improved adsorption capacity [13][14].

3.3 Adsoprtion of naphtol yellow

3.3.1 Effect of pH on adsorption capacity of naphtol yellow

The effect of pH on adsorption adsorption capacity of naphtol yellow can bee seen in **Figure 3**. The adsorption of activated carbon toward Naphthol Yellow was strongly affected by the solution pH. The highest adsorption capacity was recorded at acidic conditions % for AC-NaOH-U at pH 3, and for AC-NaOH at pH 4. At pH lower than the optimum point, the excessive H^+ ions compete with the dye molecules for the adsorption sites, thereby reducing

the electrostatic interaction between the activated carbon surface and anionic dye molecules [15].

Under acidic conditions, the activated carbon becomes protonated, resulting in positively charged adsorption sites that promote electrostatic attraction with the negatively charged sulfonate groups ($–SO_3^-$) in Naphthol Yellow [2][3]. However, at alkaline pH, the carbon surface becomes negatively charged due to deprotonation, causing electrostatic repulsion and decreased adsorption efficiency. Similar behavior has been reported in the adsorption of anionic dyes such as Naphthol AS and Naphthol AS-G [16][17][18].

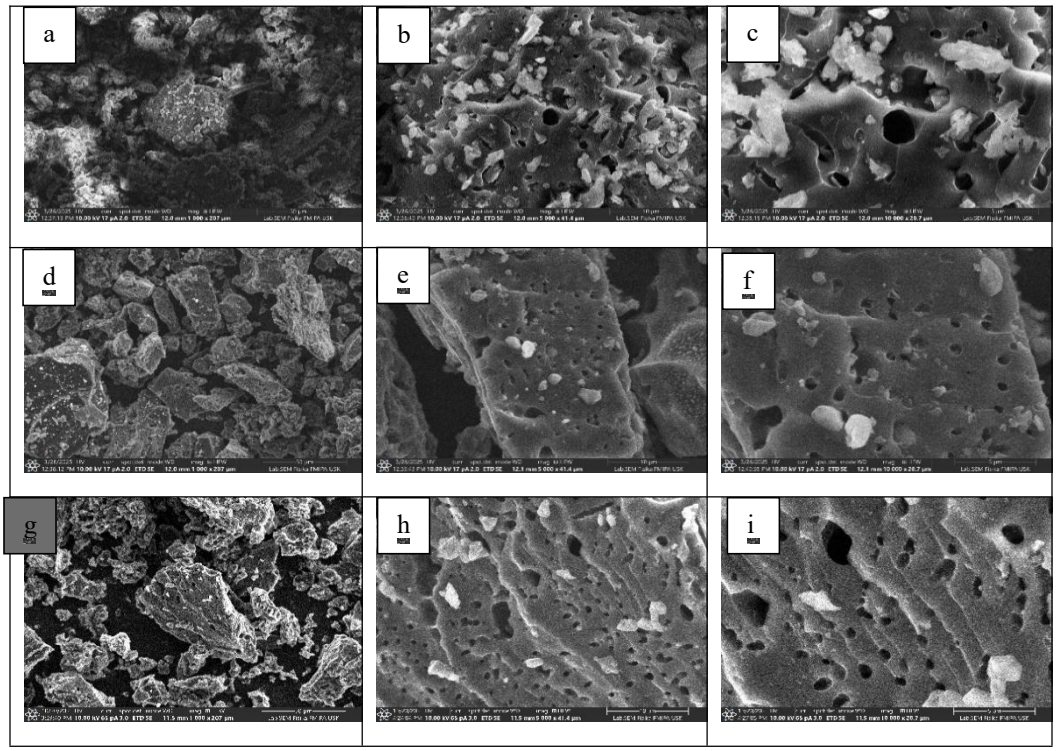

Fig. 2. Surface morphology of palm shell–based carbon under different activation conditions: (a) untreated carbon (Carbon), (b) NaOH-activated carbon (AC-NaOH), and (c) NaOH–ultrasonicated activated carbon (AC-NaOH-U).

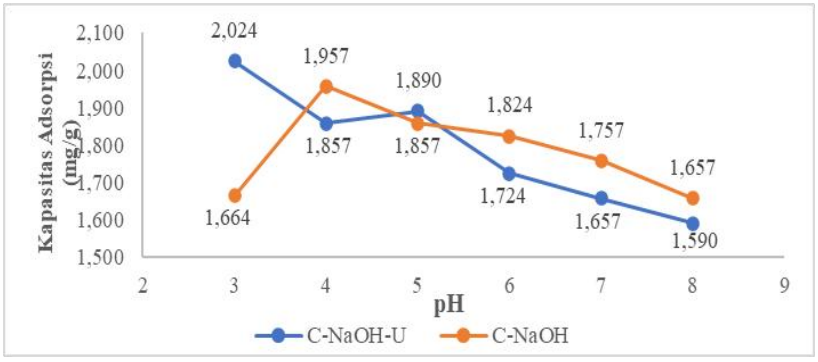

Fig. 3. Effect of pH on adsorption capacity of activated carbon samples (AC-NaOH and AC-NaOH-U).

3.3.2 Effect of contact time on adsorption capacity

The relationship between contact time and adsorption capacity is presented in **Figure 4**. The AC-NaOH-U sample reached its maximum adsorption capacity of 1.990 mg/g at 30 min, while AC-NaOH reached 1.690 mg/g at 90 min. After reaching these maximum points, adsorption capacity decreased, indicating that the active surface became saturated and some weakly bonded dye molecules desorbed back into the solution [19].

An interesting fluctuation occurred after the initial decline: adsorption capacity increased again at extended contact times. This is attributed to the slow intraparticle diffusion of dye molecules into deeper micropores, allowing the system to reach a stable adsorption equilibrium [6].

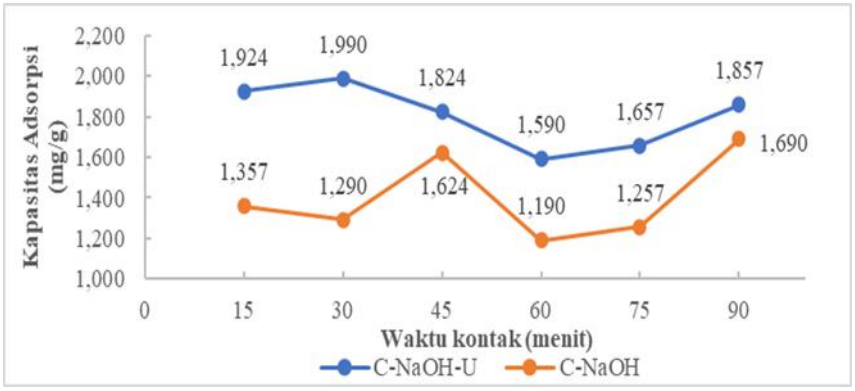

Fig. 4. Effect of contact time on adsorption capacity of AC-NaOH and AC-NaOH-U.

3.3.3 Effect of initial dye concentration on adsorption capacity

The effect of initial Naphthol Yellow concentration is shown in **Figure 5**. The adsorption capacity increased as the initial dye concentration increased from 50 to 300 ppm, consistent with the theory that a larger concentration gradient enhances mass transfer from the solution to the adsorbent surface [2][20]. At 300 ppm, the maximum adsorption capacities were 20.59 mg/g (AC-NaOH-U) and 17.59 mg/g (AC-NaOH).

The consistently superior performance of AC-NaOH-U indicates that ultrasonication enhances pore accessibility, increases pore connectivity, and accelerates diffusion into mesoporous layers [6][8]. These findings align with recent studies reporting the positive effect of ultrasonication on carbon-based adsorbents [1].

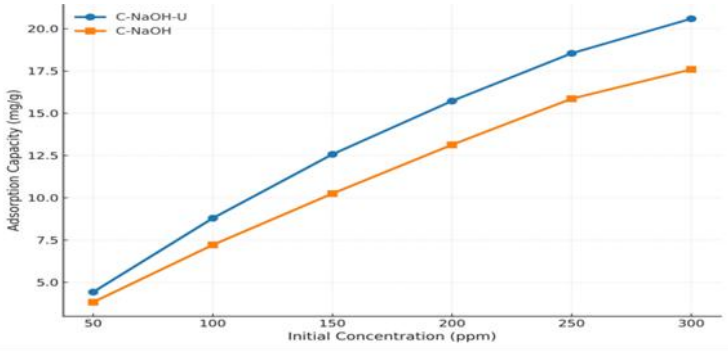

Fig. 5. Effect of initial dye concentration on adsorption capacity of AC-NaOH and AC-NaOH-U.

3.4 Illustration of adsorption

The schematic illustration depicts the adsorption behavior of dye molecules on palm shell–based carbon materials prepared under different activation conditions, namely untreated carbon (Carbon), NaOH-activated carbon (C-NaOH), and NaOH–ultrasonicated activated carbon (C-NaOH-U) can bee seen in **Figure 6**. Distinct adsorption mechanisms and efficiencies are observed as a function of surface chemistry and pore structure.

In the untreated carbon, dye adsorption is relatively limited due to the compact surface morphology and low pore accessibility. The presence of residual oxygen-containing functional groups, as indicated by FTIR analysis, contributes to weak and non-uniform interactions with dye molecules. As a result, adsorption mainly occurs on the external surface through weak physical interactions, leading to a low adsorption capacity.

Following NaOH activation, the carbon surface undergoes significant chemical and structural modification. The removal of polar functional groups and volatile components generates new micro-sized pores and increases surface roughness. These changes enhance the accessibility of adsorption sites, allowing dye molecules to penetrate into the pore structure. Adsorption in C-NaOH is therefore governed by a combination of pore filling and surface interactions, resulting in improved dye uptake compared to untreated carbon.

In contrast, the C-NaOH-U sample exhibits the most efficient adsorption behavior. The synergistic effects of chemical activation and ultrasonication produce a highly porous structure with well-developed and interconnected pores. Ultrasonication promotes deeper penetration of the activating agent and improves pore connectivity through cavitation effects, facilitating rapid diffusion of dye molecules into the internal pore network. Additionally, the increased aromaticity of the carbon framework enhances π–π interactions between the aromatic rings of the dye molecules and the carbon surface.

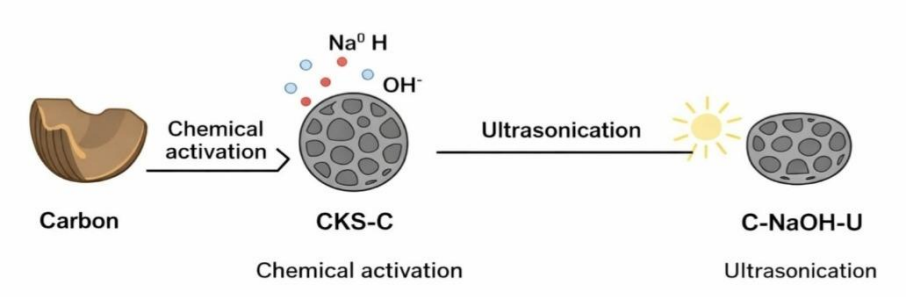

Fig. 6. Schema illustration of dye adsorption on palm shell–based carbon under different activation conditions. Untreated carbon (Carbon), NaOH-activated carbon (C-NaOH) and C-NaOH.

4 Conclusion

The combined activation method using NaOH followed by ultrasonication successfully enhanced the structural and surface characteristics of palm-shell-based activated carbon. FTIR results confirmed that chemical and ultrasonic activation effectively removed oxygen-containing functional groups and increased aromatic C=C structures, indicating a higher degree of carbon graphitization. SEM micrographs further showed a clear morphological transformation from a compact surface (raw carbon) to micro-pore formation (NaOH-activated carbon), and finally to a highly porous, interconnected structure when ultrasonication was applied.

These structural improvements directly contributed to increased surface area and porosity, which are essential for adsorption performance. Overall, the NaOH–ultrasonication activation method demonstrated superior modification capability compared to single chemical activation, making the resulting activated carbon a promising adsorbent for dye removal applications.

References

[1] Chew, T. W., H'Ng, P. S., Abdullah, L. C., Chin, K. L., Lee, C. L., et al.: A review of bio-based activated carbon properties produced from different activating chemicals during chemicals activation process on biomass and its potential for Malaysia. Materials. vol. 16, p. 7365 (2023). DOI: https://doi.org/10.3390/ma16237365

[2] Alharbi, H. A., Hameed, B. H., Alotaibi, K. D., Al-Oud, S. S., Al-Modaihsh, A. S.: Recent methods in the production of activated carbon from date palm residues for the adsorption of textile dyes: A review. Frontiers in Environmental Science. vol. 10, p. 996953 (2022). DOI: https://doi.org/10.3389/fenvs.2022.996953

[3] Bora, M., Benoy, S. M., Tamuly, J., Saikia, B. K.: Ultrasonic-assisted chemical synthesis of activated carbon from low-quality subbituminous coal and its preliminary evaluation toward supercapacitor applications. Journal of Environmental Chemical Engineering. vol. 9, p. 104986 (2021). DOI: https://doi.org/10.1016/j.jece.2020.104986

[4] Eslami, H., Khosravi, R., Miri, M. R., Gholami, A., Ghahramani, E., Khosravi, A.: Facile preparation of porous activated carbon under ultrasonic assistance for methylene blue removal: Characterization, isothermal, kinetic, and thermodynamic studies. Materials Research Express. vol. 7, p. 015620 (2020). https://iopscience.iop.org/article/10.1088/2053-1591/ab69d1

[5] Zieminska, N., Doczekalska, B. Biomass derived activated carbons in wastewater treatment – The aim of metallurgical industry. Desalination and water treatment. 318 (2024). https://doi.org/10.1016/j.dwt.2024.100320

[6] Wang, J., Li, W., Zhao, Z., Musoke, F. S. N., Wu, X.: Ultrasonic Activated Biochar and Its Removal of Harmful Substances in Environment. Microorganisms. vol. 10, no. 8, p. 1593 (2022). DOI: https://doi.org/10.3390/microorganisms10081593

[7] Murtaza, G., Ahmed, Z., Dai, D.-Q., Iqbal, R., Bawazeer, S., et al.: A review of mechanism and adsorption capacities of biochar-based engineered composites for removing aquatic pollutants from contaminated water. Frontiers in Environmental Science. vol. 10, p. 1035865 (2022). DOI: https://doi.org/10.3389/fenvs.2022.1035865

[8] Nizam, N. U. M., Hanafiah, M. M., Mahmoudi, E., et al.: The removal of anionic and cationic dyes from an aqueous solution using biomass-based activated carbon. Scientific Reports. vol. 11, p. 8623 (2021). DOI: https://doi.org/10.1038/s41598-021-88084-z

[9] Nagarajan, L., Kumaraguru, K., Saravanan, P., Rajeshkannan, R., Rajasimman, M.: Facile synthesis and characterization of microporous-structured activated carbon from agro waste materials and its application for CO_2 capture. Environmental Technology. vol. 43, no. 25, pp. 3934–3947 (2022). DOI: https://doi.org/10.1080/09593330.2021.1938243

[10] Xiang, W., Zhang, X., Chen, J., Zou, W., He, F., et al.: Biochar technology in wastewater treatment: A critical review. Chemosphere. vol. 252, p. 126539 (2020). DOI: https://doi.org/10.1016/j.chemosphere.2020.126539

[11] Yimin, R., Abla, R., Dawut, G., Abdukayum, A and Xiong, B. Preparation and Adsorption Performance of Walnut Waste-Based Magnetic Activated Carbon with High Specific Surface Area. ACS Omega, 10, 498−508 (2025). https://doi.org/10.1021/acsomega.4c05032

[12] Ibrahim, M. H., El-Naas, M. H., Zhang, Z., Van der Bruggen, B.: Activated carbon from biomass waste precursors: Factors affecting production and adsorption mechanism. Chemosphere. vol. 294, p. 133764 (2022). DOI: https://doi.org/10.1016/j.chemosphere.2022.133764

[13] Zhi, K., Zhang, J., Zhang, J et al. Application of biochar-based materials as adsorbents for aquatic environment remediation: Preparation, mechanisms, and performance evaluation. J. Hazardous Materials Advances. 23 (2026). https://doi.org/10.1016/j.hazadv.2026.101321

[14] Yan, Q., Nosratabad, N.A., Du et al. Highly effective lead removal by novel alkaline biochar prepared by pyrolysis of woody biomass impregnated with low-level NaOH. J. Hazardous Materials Advances. 18 (2025). DOI : https://doi.org/10.1016/j.hazadv.2025.100657

[15] Vojnović, B., Cetina, M., Franjković, P., Sutlović, A.: Influence of Initial pH Value on the Adsorption of Reactive Black 5 Dye on Powdered Activated Carbon: Kinetics, Mechanisms, and Thermodynamics. Molecules. vol. 27, no. 4, p. 1349 (2022). DOI: https://doi.org/10.3390/molecules27041349

[16] Dutta, S., Gupta, B., Srivastava, S. K., Gupta, A. K.: Recent advances on the removal of dyes from wastewater using various adsorbents: A critical review. Materials Advances. vol. 2, pp. 4497–4531 (2021). DOI: https://doi.org/10.1039/D1MA00354B

[17] Lin, X., Zhou, Q., Xu, H., Chen, H., Xue, G.: Advances from conventional to biochar enhanced biotreatment of dyeing wastewater: A critical review. Science of the Total Environment. vol. 907, p. 167975 (2024). DOI: https://doi.org/10.1016/j.scitotenv.2023.167975

[18] Yang, N., Jun, B.-M., Choi, J. S., Park, C. M., Jang, M., et al.: Ultrasonic treatment of dye chemicals in wastewater: A review. Chemosphere. vol. 354, p. 141676 (2024). DOI: https://doi.org/10.1016/j.chemosphere.2024.141676
[19] Kalsoom, Ali, A., Khan, S., Ali, N., Khan, M. A.: Enhanced ultrasonic adsorption of pesticides onto the optimized surface area of activated carbon and biochar: Adsorption isotherm, kinetics, and thermodynamics. Biomass Conversion and Biorefinery. vol. 14, pp. 15519–15534 (2023). DOI: https://doi.org/10.1007/s13399-023-04170-4
[20] Premarathna, K.S.D., Rajapaksha, A.U., Sarkar, B et al. Biochar-Based Engineered Composites for Sorptive Decontamination of Water : A Review. Chemical Engineering. (2019). https://doi.org/10.1016/j.cej.2019.04.097